

RECENT PROGRESS IN NANOSCALE INDENTATION OF POLYMERS USING THE AFM

by

M. VanLandingham and J. Villarrubia
Building and Fire Research Laboratory
National Institute of Standards and Technology
Gaithersburg, MD 20899, USA

and
G. Meyers
Dow Chemical Company
1897E Building
Midland, MI 48677, USA

Reprinted from the SEM IX International Congress on Experimental Mechanics.
Proceedings. Society for Experimental Mechanics. June 5-8, 2000, Orlando, FL, 912-915 pp,
2000.

NOTE: This paper is a contribution of the National Institute of Standards and
Technology and is not subject to copyright.



NIST

National Institute of Standards and Technology
Technology Administration, U.S. Department of Commerce

Recent Progress in Nanoscale Indentation of Polymers Using the AFM

M. VanLandingham*, J. Villarrubia*, and G. Meyers**

* National Institute of Standards and Technology, 100 Bureau Drive, Gaithersburg, MD 20899

** The Dow Chemical Company, Analytical Sciences, 1897E Building, Midland, MI 48667

ABSTRACT

For reliable indentation measurements, knowledge of the shape of the indenter tip is required. For indentation measurements involving sub-micrometer scale contacts, accurate characterization of the tip shape is difficult. In this paper, a technique referred to as blind reconstruction is used to measure the tip shapes of two probes used with the atomic force microscope (AFM) to indent polymeric materials. This method has the potential for material independent calibration of indenter tips. Initial results from blind reconstruction are compared to results of a tip shape calibration method in which a reference material of known modulus is indented using a range of applied loads. Discrepancies between the two sets of results are discussed in terms of experimental uncertainties.

1 INTRODUCTION

A number of depth-sensing indentation devices have been developed recently that allow the amount of penetration of an indenter into a material to be measured as a function of load during both the loading and unloading sequence [1-3]. Many of these devices produce indentation sizes and depths with sub-micrometer dimensions for hard materials (e.g., single-crystal silicon, hardness = 14 GPa [3]). The objective of micro- and nanoindentation testing using these devices is to produce absolute measurements of material properties under indentation loading. Further, the ability of these devices to measure the responses of microscopic regions can be a key to understanding mechanical behavior of technologically important material systems. However, some polymers are so soft that the material response cannot be measured at all with these devices because the system compliance is too low [4]. Even for stiffer polymers (modulus values greater than 1 GPa), producing indents with both lateral and depth dimensions much less than 1 μm is difficult, particularly because these devices cannot detect initial contact loads less than 1 μN . Thus, these systems have limited capabilities for studying polymer thin films, polymer composites, and other important polymer systems.

The atomic force microscope (AFM) is particularly useful for evaluating polymeric materials on a sub-micrometer scale. The AFM employs a probe consisting of a sharp tip (nominal tip radius on the order of 10 nm) located near the end of a cantilever beam that is scanned across the sample surface using piezoelectric scanners. The AFM can also be operated in a non-imaging mode, called force mode, to

perform indentation tests. A force curve is produced, which is a plot of tip deflection as a function of the vertical motion of the scanner. This curve can be analyzed to provide information on the local mechanical response [5-7]. Also, the spring constant of the cantilever probe can be chosen such that small differences in response can be detected for polymers having a certain range of stiffness corresponding to the chosen spring constant [5].

AFM indentation measurements are relative measurements, largely due to the lack of information regarding the tip shape of the AFM probes. Also, current tip shape calibration procedures used in depth-sensing indentation rely on indentation results from a reference material, and the reproducibility of these methods has been poor in a recent interlaboratory comparison [8]. In this paper, a technique referred to as blind reconstruction is used as a material-independent method for characterizing the tip shapes of probes used with the AFM to indent polymeric materials. Results using this method are compared to results of a material-dependent tip shape analysis.

2 EXPERIMENTAL

2.1 Materials

A benzocyclobutene (BCB) polymer (Cyclotene 5021, The Dow Chemical Company [9]) was prepared by the manufacturer as a smooth film by spin casting from a partially cured (B-stage) solution in mesitylene onto a thermal oxide silicon wafer. The B-staged material had been taken to a state of 40% cure with a mass fraction of solids of 0.63. Spin casting at 323 rad/s (3085 rpm) for 30 s was followed by curing at 250 $^{\circ}\text{C}$ for 60 min, all in a nitrogen atmosphere. Film thickness was measured using ellipsometry to be $10.99 \mu\text{m} \pm 0.37 \mu\text{m}$. From AFM results utilizing phase contrast imaging, heterogeneity in this sample was not observed, and root-mean-square roughness, measured using $5 \mu\text{m} \times 5 \mu\text{m}$ AFM images, was found to be $6 \text{ nm} \pm 0.5 \text{ nm}$. The room-temperature tensile modulus was reported by the manufacturer to be approximately 2.9 GPa and the glass transition temperature, measured using differential scanning calorimetry, was in excess of 350 $^{\circ}\text{C}$.

2.2 Indentation with the AFM

Indentation of the BCB polymer sample was performed using two different AFM indentation systems. The first system was a Dimension 3100 AFM (Digital Instruments) [9]. A diamond-

ipped stainless steel cantilever was used as the indentation probe using a technique described in detail elsewhere [5-7]. The spring constant of this probe was measured by the manufacturer (Digital Instruments [9]) to be $120 \text{ N/m} \pm 10 \text{ N/m}$. Three sets of indentation measurements were made with each set containing one indent at eight load levels ranging from $1.4 \mu\text{N}$ to $13.7 \mu\text{N}$. The measured load-penetration responses at each force level were used to produce an estimation of the tip shape using indentation tip shape calibration procedures (see Reference 1).

The second system was a Triboscope (Hysitron) [9] depth-sensing indentation system mounted on a Multimode AFM (Digital Instruments) [9]. When interfaced with an AFM, the transducer/indenter tip assembly replaces the AFM cantilever probe assembly. A diamond indentation tip with Berkovich geometry was used for imaging and indentation. Imaging was performed with this tip in contact with the sample under a constant applied load of approximately $1 \mu\text{N}$, as measured by the transducer and used as feedback to the AFM scanner. Tip shape calibration (see Reference 1) was performed by analyzing a set of 28 load-penetration curves on fused silica with maximum loads of between $25 \mu\text{N}$ and $5200 \mu\text{N}$. For most of the load levels, two or more load-penetration curves were analyzed. Indentation of the BCB sample was then performed using maximum loads similar to those used for tip shape calibration.

Prior to the tip shape calibration measurements, the compliance of the load frame was also calibrated for both indentation systems [1]. This calibration allows the displacement of the load frame to be removed from the total measured displacement so that only displacement due to penetration of the tip into the sample remains. For the AFM cantilever probe, a sample that is stiff with respect to the probe is used so that no tip penetration occurs. The measured force-displacement response is thus characteristic of the AFM probe and the particular operating conditions. This probe response can be removed from the force-displacement responses measured on the polymer sample so that only the force-penetration response remains [5-7]. For each of the eight load levels used to indent the BCB sample, 10 force curves were obtained on a smooth sapphire sample, five directly before and five directly after indenting the BCB sample, using the same probe and operating conditions. For the depth-sensing indenter, load frame compliance was calibrated by indenting fused silica, at load levels ranging from $3000 \mu\text{N}$ to $5200 \mu\text{N}$ using the manufacturer's recommended procedure. A total of 11 load-penetration curves were analyzed.

2.3 Blind Reconstruction

Blind reconstruction takes advantage of the "self-imaging" that is always present in an AFM topographic image [10]. At each pixel in any image, information is contained about the tip geometry as well as the sample surface. In fact, all image protrusions can be regarded as tip images, each broadened in different ways by the different underlying surface features. The purpose of blind reconstruction is to extract the part concerning the tip, which begins by modeling topographic AFM imaging as follows: (1) a sharp tip is positioned above the sample at lateral coordinates (x, y) ; (2)

the tip is lowered until some part of it makes contact with some part of the sample; and (3) the relative vertical position, i , is recorded for all (x, y) of interest, usually in raster-scanned order, and the resulting $i(x, y)$ is the image. As has been widely recognized [11-13], this model can be economically expressed in terms of the set of points, I , on or below the image surface, a similar set of points, S , describing the sample, the set of points, P , describing the reflection of the tip through the origin, and the mathematical morphology dilation operator, \oplus :

$$I = S \oplus P \quad (1)$$

To the extent that this model is realistic, the tip geometry can be determined from an unknown experimental sample's image [11, 12]. However, the tip shape determined after consideration of all image points is an outer bound on the true tip shape, and the sharpest features on the specimen determine the accuracy of the 3-dimensional tip shape information. Also, Eq. (1) is assumed to be a good model for topographic imaging. In practice, the dilation model is an approximation, as the real image includes non-tip artifacts such as noise, scanner nonlinearity, and feedback loop response time. These instrumental artifacts produce sharp spikes on the image that cannot be entirely removed by filtering. To limit the influence on the tip estimate of these small deviations from the model, a threshold parameter is used that describes the maximum amount, by which the image deviates from an ideal dilation [13].

2.4 AFM imaging of tip shape characterizers

AFM images of three samples, which are often referred to as tip shape characterizers, were used to estimate the shapes of indenter tips using blind reconstruction. Imaging was performed with a diamond-tipped stainless steel cantilever probe in tapping mode, and also with the Berkovich indenter tip in contact mode. Images with scan sizes of $1 \mu\text{m} \times 1 \mu\text{m}$, $3 \mu\text{m} \times 3 \mu\text{m}$, and $5 \mu\text{m} \times 5 \mu\text{m}$ consisting of 512 scan lines, each line with 512 pixels, and taken at a scan rate of 1 Hz, were made for each tip-sample combination. Two of the samples, described as roughness-type characterizers, were rough columnar thin films of niobium (Nb) and titanium (Ti), respectively (General Microdevices [9]). The sharpest features for the Nb specimen have a radius of approximately 2 nm (manufacturer's specification), while the Ti sample has somewhat blunter but taller features. However, the largest features are not particularly large, and thus images of these samples were used only to reconstruct a portion of the tip near the apex. The other sample was a silicon grating (ND-MDT [9]) that contained an array of spike-like features with symmetric tip sides, a tip angle of less than 20° , and a tip radius of curvature of less than 10 nm (manufacturer's specifications). The image of a spike is a 3-dimensional image of the AFM tip that is blunted by the size of the spike. Because the spike features are tall, this sample was used to reconstruct the portion of the tip away from the apex that was not accessible to the roughness samples.

3 RESULTS AND DISCUSSION

An image created by scanning the spike-type tip characterizer sample with the Berkovich tip is shown in

Figure 1a. The spikes essentially image the tip such that the Berkovich tip geometry, broadened by the finite size of each spike, is produced several times in the image. The area-depth relationship for this tip was calculated from blind reconstruction results. In Figure 1b, this result is compared to that from an indentation tip-shape analysis, in which fused silica was indented at a variety of loads and penetration depths with this same Berkovich tip.

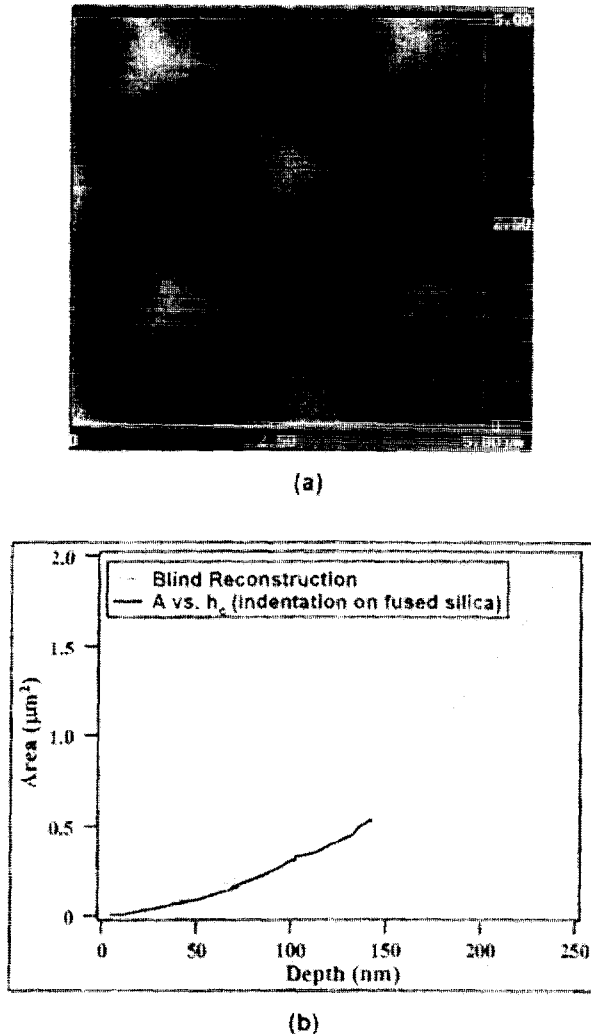


Figure 1 -- (a) an AFM topographic image generated by scanning a spike-type characterizer sample with a Berkovich indentation tip (color contrast from black to white represents a total range of 800 nm), and (b) a plot of the area-depth relationship for the Berkovich tip in which blind reconstruction results are compared to results from an indentation tip-shape analysis.

In a similar study, the diamond-tipped AFM cantilever was used to scan the tip characterizer samples and indent the BCB polymer at a variety of loads and penetration depths. An AFM image of the plastic impressions left in the polymer is shown in Figure 2a and the load-indentation depth curves corresponding to one row of indents is shown in Figure 2b. In Figure 2c, the area-depth relationships calculated from the

blind reconstruction results and from a tip-shape analysis using the polymer indentation results are compared.

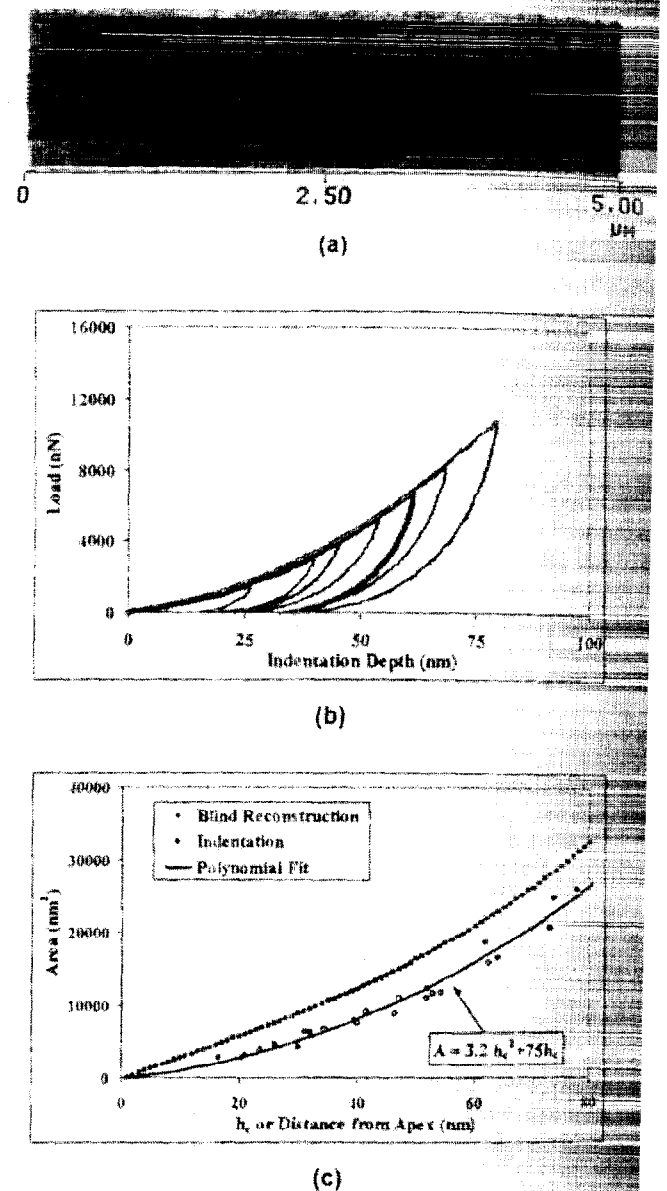


Figure 2 -- (a) an AFM topographic image showing three rows of indents made on the polymer sample, each row containing indents produced at eight different loads (color contrast from black to white represents a total range of 20 nm); (b) a load-indentation depth plot for one of the rows in (a); and (c) a plot of the area-depth relationship for the AFM diamond tip in which blind reconstruction results are compared to results from an indentation tip-shape analysis.

In both Figures 1b and 2c, significant discrepancies are observed between the two methods of tip shape characterization. However, these results are preliminary, and a thorough analysis of measurement uncertainties for the two methods has yet to be completed. Uncertainties in the blind reconstruction results include (1) the sizes of the sharpest features of the characterizer samples, particularly

with regard to the spike characterizer, which may be more susceptible to damage during imaging; (2) non-tip image artifacts and the choice of the threshold parameter used to reduce the influence of those artifacts; and (3) for the depth-sensing indenter, slight deviations from perpendicularity of the tip with respect to the characterizer sample.

In general, uncertainties in the blind reconstruction area measurements in Figures 1b and 2c are estimated to be less than $\pm 5\%$ of each calculated value, although current efforts involve a more complete uncertainty analysis. However, the uncertainties in the indentation tip shape analyses could be much larger [6, 8]. For the depth-sensing indenter, these uncertainties include (1) load-frame compliance calibration; (2) detection of a true zero in load and displacement; (3) uncertainties associated with curve fitting; (4) uncertainties in the elastic modulus of fused silica; (5) and uncertainties related to differences between elasticity theory and real material behavior. For the AFM, uncertainties include (1) lateral forces acting on the tip due to cantilever bending; (2) scanner and photodiode nonlinearities; (3) uncertainties associated with curve fitting; and (4) time-dependent deformation behavior of the polymer.

Direct comparisons between the two methods of tip shape calibration are not possible until complete uncertainty analyses of the indentation measurements are available. Interestingly, however, measurements of elastic modulus, E , for the BCB polymer were made using both the depth-sensing indenter and the AFM. For the AFM, $E = 2.1 \text{ GPa} \pm 0.2 \text{ GPa}$ using the blind reconstruction results. For the depth-sensing indenter, $E = 3.7 \text{ GPa} \pm 0.2 \text{ GPa}$ using the indentation tip shape calibration. In both cases, the uncertainty expressed is the estimated standard deviation from numerous indentation measurements. The tensile modulus measured by the manufacturer was $E = 2.9 \text{ GPa}$. Thus, both sets of indentation measurements are in reasonable agreement with the bulk tensile measurement.

4 SUMMARY AND CONCLUSIONS

In this study, blind reconstruction was used to estimate the shape of an AFM diamond probe tip and a tip with Berkovich geometry used with AFM-based indentation systems. In both cases, large deviations were observed between area functions measured using blind reconstruction and those measured using indentation tip-shape calibration. These differences might be due to large uncertainties in the indentation measurements. However, direct comparisons between the two methods of tip shape calibration are not currently possible due to incomplete uncertainty analyses.

REFERENCES

- [1] Oliver, W. C. and Pharr, G. M., *An improved technique for determining the hardness and elastic modulus using load and displacement sensing indentation experiments*, Journal of Materials Research, **7**(6), pp. 1564-1583, 1992.
- [2] Corcoran, S. G., Colton, R. J., Lilleodden, E. T., and Gerberich, W. W., *Anomalous plastic deformation at surfaces: nanoindentation of gold single crystals*, Physical Review B, **55**(24), pp. 57-60, 1997.
- [3] Doerner, M. F. and Nix, W. D., *A method for interpreting the data from depth-sensing indentation instruments*, Journal of Materials Research, **1**(4), pp. 601-609, 1986.
- [4] Lucas, B. N., *Mechanical characterization of sub-micron polytetrafluoroethylene (PTFE) thin films*, Thin-Films -- Stresses and Mechanical Properties VII, Vol. 505, Materials Research Society, pp. 97-102, 1998.
- [5] VanLandingham, M. R., McKnight, S. H., Palmese, G. R., Elings, J. R., Huang, X., Bogetti, T. A., Eduljee, R. F., and Gillespie Jr., J. W., *Nanoscale indentation of polymer systems using the atomic force microscope*, Journal of Adhesion, **64**(1-4), pp. 31-59, 1997.
- [6] VanLandingham, M. R., *The effect of instrumental uncertainties on AFM indentation measurements*, Microscopy Today, Issue No. 97-10, pp. 12-15, 1997.
- [7] VanLandingham, M. R., Dagastine, R. R., Eduljee, R. F., McCullough, R. L., and Gillespie, Jr., J. W., *Characterization of nanoscale property variations in polymer composite systems: part 1 -- experimental results*, Composites-A, **30**(1), pp. 75-83, 1999.
- [8] Jennett, N. M. and Meneve, J., *Depth sensing indentation of thin hard films: a study of modulus measurement sensitivity to indentation parameters*, Fundamentals of Nanoindentation and Nanotribology, Vol. 522, Materials Research Society, pp. 239-244, 1998.
- [9] Certain commercial instruments and materials are identified in this paper to adequately describe the experimental procedure. In no case does such identification imply recommendation or endorsement by the National Institute of Standards and Technology, nor does it imply that the instruments or materials are necessarily the best available for the purpose.
- [10] Montelius, L. and Tegenfeldt, J. O., *Direct observation of the tip shape in scanning probe microscopy*, Applied Physics Letters, **62**(21), pp. 2628-2630, 1993.
- [11] Villarrubia, J. S., *Morphological estimation of tip geometry for scanned probe microscopy*, Surface Science, **321**(3), pp. 287-300, 1994.
- [12] Bonnet, N., Dongmo, S., Vautrot, P., and Troyon, M., *A mathematical morphology approach to image-formation and image-restoration in scanning tunneling and atomic-force microscopies*, Microscopy, Microanalysis, and Microstructures, **5**(4-6), pp. 477-487, 1994.
- [13] Villarrubia, J. S., *Algorithms for scanned probe microscope image simulation, surface reconstruction, and tip estimation*, Journal of Research of the National Institute of Standards and Technology, **102**(4), pp. 425-454, 1997.